Electrochemical Reduction of Mn (II) Mediated by C_{60}/Li$^+$ Modified Glassy Carbon Electrode

M. M. Radhi[*], *W. T. Tan, M. Z. B Ab Rahman, and A. B. Kassim*

Department of Chemistry, Faculty of Science, University Putra Malaysia, 43400, UPM, Serdang, Selangor, Malaysia
[*]E-mail: mmrchm2007@yahoo.com

Glassy carbon electrode (GCE) was modified with C_{60} (C60/GCE) by a solution evaporation technique, C_{60}/Li$^+$/GCE was prepared by modifying C_{60}/GCE in Li+ solution via cv potential cycling.Two reduction peaks of Mn(II), which appear at +600 and -100 mV vs Ag/AgCl at GC electrode increased considerably with slight peak shifting when the two modified GCE electrodes were used. The sensing characteristics of the modified film electrodes, demonstrated in this study comprised of: (i) a wide working potential window ranging from +1.8 to -1.8V (depending on different scan rate, pH, concentration and temperature); (ii) a wide applicable pH range (at least from 2 to 11); (iii) a wide applicable temperature range 30-90°C; (iv) a satisfactory linear voltammetric and amperometric response to various analytes; (v) good reproducibility; (vi) Other heavy metal ions such as Hg^{2+}, Cd^{2+} and Cu^{2+} appear to exert positive interference on the reduction peaks of Mn^{2+} and (vii) stable and fast current response . The reduction current response of Mn(II) at C_{60}/Li$^+$/GCE is also significantly dependent on pH, temperature, concentration and scan rate. Based on the surface charge determined by chronocoulometry (CC), C_{60}/Li$^+$/GCE appears more conductive in acidic solution than in alkaline. Based on Cottrell equation, diffusion coefficient of 5.12x 10^{-6}cm^2/sec for the reduction of Mn^{2+} was determined.

1. INTRODUCTION

The electrochemistry of C_{60} in the solution phase voltammetry has been studied and also in solid phase [1-6]. From the experimental data which challenges the model proposed since the mid-1990s that the reduction of C_{60} films in aqueous electrolytes involves the formation of $M^{+n}C_{60}^{n-}$ where M^+ represents a metal cation or proton. It provides by voltammetric evidence that the reduction of C_{60}

films in aqueous media is instead the reduction of adventitious poly-epoxidated $C_{60}O_n$ with subsequent chemically irreversible loss of O^{2-} as water, and that C_{60} is not reduced within the potential windows of aqueous electrolytes [7].

Solution cast films of C_{60} on glassy carbon substrates were studied in aqueous solutions as possible electrode materials. These films could be reduced in 1 M NaOH solutions to become conductive, possibly due to the formation of Na_xC_{60}. Both the reduction and the oxidation processes were completely irreversible [8].

Solution cast C_{60} films were studied in aqueous solutions containing a variety of doping cations Li^+, Na^+, K^+, Rb^+, Cs^+, Ca^{2+}, and Ba^{2+}. The reduction peak potentials also changed with the concentration of the cations, and this was assumed to be the consequence of the formation of reduced films which acted as cation exchange membranes. The most active and stable were those formed with K^+ and Rb^+ dopants. Some of the doped films with Li^+, Na^+ and Ba^{2+} could be oxidized electrochemically, while the others were probably oxidized only on their surfaces [9]. The usefulness of a C_{60}-fullerene modified gold (Au) electrode in mediating the oxidation of methionine in the presence of potassium ions electrolyte has been demonstrated. During cyclic voltammetry, an oxidation peak of methionine appearing at +1.0 V vs. Ag/AgCl was observed. The oxidation current of methionine is enhanced by about 2 times using a C_{60} modified gold electrode. The current enhancement is significantly dependent on pH, temperature and C_{60} dosage [10].

Voltammetric studies on C_{60} fullerene particles adhered to an electrode surface by solvent casting or mechanical transfer exhibit evidence of nucleation and growth controlled processes for the $C_{60}{}^{0/-}$ and $C_{60}{}^{-/2-}$ solid state when the modified electrode is in contact with acetonitrile solutions containing $NBu_4{}^+$ electrolyte. Although peak potentials and peak separations are dependent on scan rate as well as the amount of deposit and temperature, potentials obtained using a zero-current extrapolation method are almost independent of all these parameters [11].

Some manganese potentialities for modification of solid-state electrodes are exploited. It is based on the ability of Mn^{2+} to incorporate easily onto the thin lipid films, deposited at the electrode surface. The voltammetric analysis of thus modified glassy carbon electrodes (GCE) reveals possibilities for driving redox reactions in the electrolyte. The results suggest a transfer of electrons across the lipid phase mediated through the transitions of the embedded manganese. On the other hand, at higher concentrations the Mn^{2+} integration within the supported liquid films leads to changes in their structural parameters. In this respect, a comparison with the action of Ca^{2+} and Mg^{2+} shows a some what stronger impact of the Mn^{2+} ions [12].

In application of Mn^{2+} in MRI-visible paramagnetic tracers to reveal in vivo connectivity can provide important subject-specific information for multisite, multielectrode intracortical recordings in combined behavioral and physiology experiments. In other words, used as a paramagnetic MRI tracer, Mn^{2+} can permit the visualization of neural networks covering at least four processing stages [13].

The employment of Mn^{2+} as a mediator for the electron transfer across glassy carbon-supported thin lecithin films in contact with electrolyte is studied; the results suggest that the ascorbate oxidation, which is normally hampered by the film, can proceed through the incorporated manganese. In this respect, the potential of Mn^{2+} for modification of lipid wetting films in construction of sensitive interfaces is founded [14].

In this work, C_{60} modified Mediators are fixed on the GC electrode surface using different methods such as C_{60} and C_{60}/Li^+ electrodes. Results have been shown the modified electrode C_{60}/Li^+ has good electrochemical behavior in term of stability and high sensitivity for the detection of some heavy metal ions.

2. EXPERIMENTAL PART

2.1. Chemicals and materials

C_{60} (Fluka, 98%, HPLC) and all reagents were analytical reagent or electrochemical grade purity. All solutions were prepared using distilled water. Unless otherwise specified, the supporting electrolyte was 0.1 M KCl in aqueous media at room temperature.

2.2. Methods

Electrochemical workstations of Bioanalytical system Inc. USA: Models BAS CV 50W with potetiostate driven by electroanalytical measuring softwares was connected to PC computer to perform cyclic voltammetry (CV), chronocoulometry (CC) and chronoamperometry (CA). An Ag/AgCl (3M NaCl) and Platinum wire were used as a reference and counter electrode respectively. The working electrode used in this study were GCE, C_{60}/GCE obtained by evaporated C_{60} on GCE using acetonitrile as a solvent, and C_{60}/Li^+/GCE by modified C_{60}/GCE with 0.1M LiOH using cyclic voltammetry.

2.3. Preparing a C_{60} – modified electrode

A solution evaporation technique was employed [15-16]. It was done by evaporating a certain quantity (µL) of C_{60} solution onto the clean GCE surface. The solution of C_{60} was prepared by dissolving C_{60} in acetonitrile to form a brownish solution. A 20µL solution was then deposited onto GCE by successive fast drying of the C_{60} droplets to produce an array of microcrystals of fullerene. C_{60}/Li^+/GCE was prepared by the doping of Li^+ ion on to C_{60}/GCE via 10 potential cycling between +600 to -600mV in presence of 0.1M LiOH during cyclic voltammetry.

2.4. Scanning Electron Microscopy

Scanning Electron Microscopy (SEM) was used to examine the morphology of the C_{60} microcrystals attached to a graphite electrode surface. SEM of C_{60} attached via solvent cast on to 5mm diameter basal plane graphite electrode exhibits an array of microcrystals (Fig. 1a). After controlled potential electrolysis was carried out in the presence of Mn(II), the size increased slightly attributing to the presence of reduced Mn(II) species and the hydration effect.
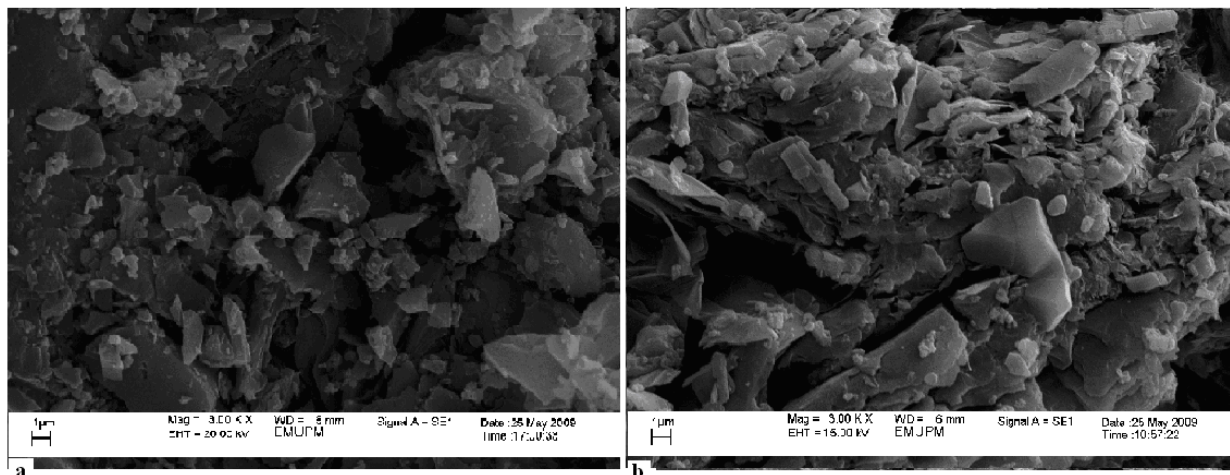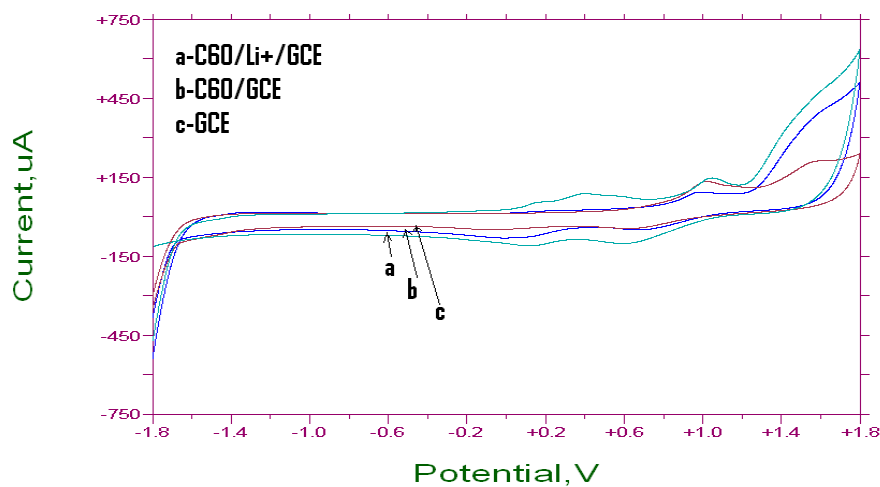
Figure 1. Scanning Electron Microscopy (SEM) of the C_{60} microcrystal attached to a graphite electrode surface. (a) SEM of C_{60} attached via solvent cast on to 5mm diameter basal plane graphite electrode before electrolysis (b) SEM of C_{60} after electrolysis in Mn(II) solution by cyclic voltammetry.
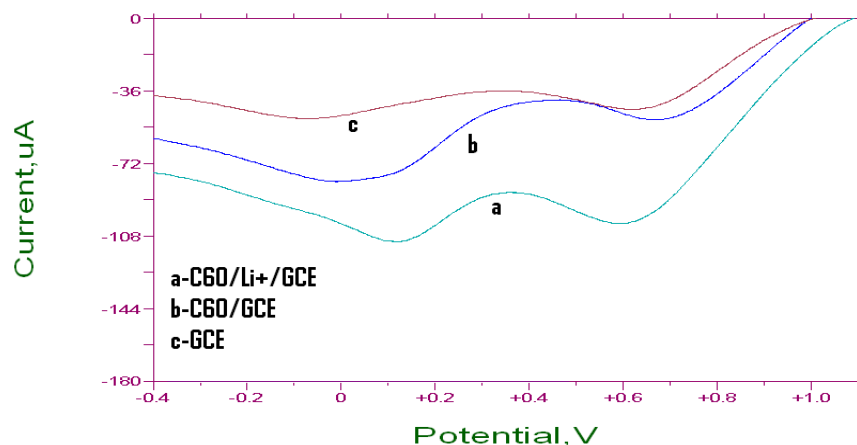
3. RESULTS AND DISCUSSION

3.1. Effect of different modified electrodes

Figure 2(a) and (b) show the reduction peaks of Mn^{2+} was considerably enhanced by 4-5 times with about 200mV peak shifting towards origin when C_{60} /Li^+/GCE was used in comparison with C60/GCE and GCE. Evidently degree of sensitivity response increases in the order of: C_{60}/Li^+/GCE > C_{60}/GCE > GCE.

(A)

(B)

Figure 2. (A) cyclic voltammogram of 1mM Mn^{2+} in 0.1M KCl as supporting electrolyte at scanning rate 100 mv s^{-1} using (a) $C_{60}/Li^+/GCE$ (b) C60/GCE and (c) GCE versus Ag/AgCl. **(B)** Enlarged voltammogram for the reduction peak of 1mM Mn^{2+} in 0.1M KCl as supporting electrolyte at scanning rate 100 mv s^{-1} using (a) $C_{60}/Li^+/GCE$ (b) C60/GCE and (c) GCE versus Ag/AgCl.

The reduction peaks of Mn^{2+} appears more discernable when C_{60}/GC electrode is used as compared with bare GC electrode. Reduction peaks become even more pronounced and enhanced by 4-5 times at the electrode surface of $C_{60}/Li^+/GCE$. The observation of one or two reduction peaks (+600 and +100mV) appears to be dependent on pH, and temperature conditions.

3.2. Optimization of conductive effect

3.2.1. Effect of varying pH

The two pH media are in acidic solution at pH from 2 to 6, and in alkaline solution at pH from 5 to 11 exhibit distinct differences in the reduction processes of Mn(II) at $C_{60}/Li^+/GC$ electrode surface.

(a)Acidic solution of pH 2-6:

Acidic pH solution was varied from 2 to 6 to determine its effect on the electrocatalytic reduction of Mn^{2+} at the C_{60}/Li^+ modified GC electrode. It was observed that the reduction current of Mn^{2+} gradually and linearly increases with lowering of pH from 6 to 2 accompanied by a linear shift in reduction potential which satisfies the linear equation of I(uA)= -145.68 pH + 688.6 with correlation coefficient of $R^2=0.948$ and E(mV)= - 54.23 pH + 682.5 with correlation coefficient of $R^2=0.9121$. The two reduction peaks of Mn^{2+} at +600 and +100mV the second peak was shifted to a more negative potential of -1000mV with increased current, for both the reduction peaks on different modified electrodes as shown in Figure 3. The mechanism of the reduction steps is explained as follow:

$$Mn^{2+} + e \longrightarrow Mn^+ \qquad E = +600mV \qquad (1)$$

$$Mn^+ + e \longrightarrow Mn \qquad E = - 145\ mV \qquad (2)$$

On the other hand, the potential of the reduction peak of Mn^{2+} to $Mn(0)$ value is explained as follow [17]:

$$Mn^{2+} + 2\,e \longrightarrow Mn \qquad\qquad E = -118\ mV \qquad (3)$$
$$Mn^{3+} + e \longrightarrow Mn^{+2} \qquad\qquad E = +154\ mV \qquad (4)$$

(b) Alkaline solution of pH 7 to 11:

In basic media, the reduction peaks of Mn^{2+} exhibits different voltammetric behaviors. The first reduction peak was shifted to higher oxidation potential at +700 mV, while the second peak is still in the same potential of +100mV with increasing current, in this pH the Mn^+ ion was converted to $Mn(0)$ as in equation 2. Figure 4 shows that at pH 11, the first reduction peak increased significantly in the presence of the modified GC electrodes..
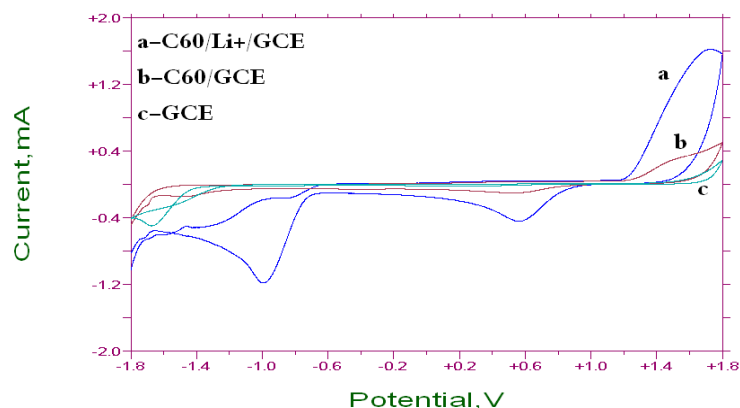

Figure 3. Cyclic voltammogram of effect pH 2 on 1mM Mn^{2+} in 0.1M KCl at pH 2, using (a) $C_{60}/Li^+/GCE$ (b)C_{60}/GCE and (c) GCE versus Ag/AgCl, 100mV s^{-1}.

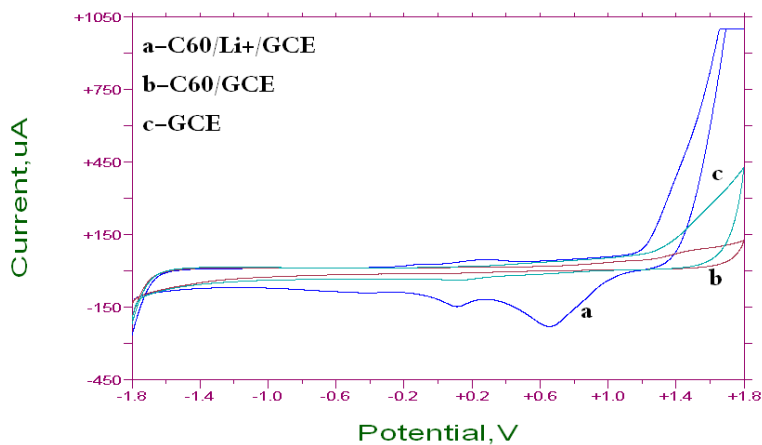**Figure 4.** Cyclic voltammogram of 1mM Mn^{2+} in 0.1M KCl at pH 11, using (a) $C_{60}/Li^+/$ GCE (b) C_{60}/GCE and (c) GCE versus Ag/AgCl, 100mV s^{-1}.

3.2.2. Effect of varying Temperature

Effect of temperature on the reduction process of Mn^{2+} was studied. The current increases gradually at the temperature of 30 to 90^oC. Figure 5 is plot of log Ipc (reduction current) of Mn^{2+} versus reciprocal of temperature which is found to be fairly linear in agreement with thermodynamic expectation of Arrhenious equations 5 and 6 [11].

$$\sigma = \sigma^o \, Exp\,(- E_a/\,RT\,) \tag{5}$$
$$D = D^o \, Exp\,(-E_a/\,RT) \tag{6}$$

Where σ / D are conductivity / diffusibility and σ^o /D^o are standard conductivity / the initial diffusibility.
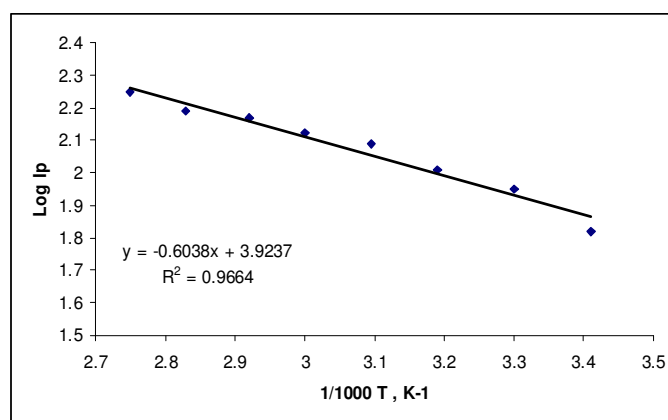

Figure 5. Dependence of reduction current of Mn^{+2} as a function of Temperature at $C_{60}/Li^+/GCE$ versus Ag/AgCl.
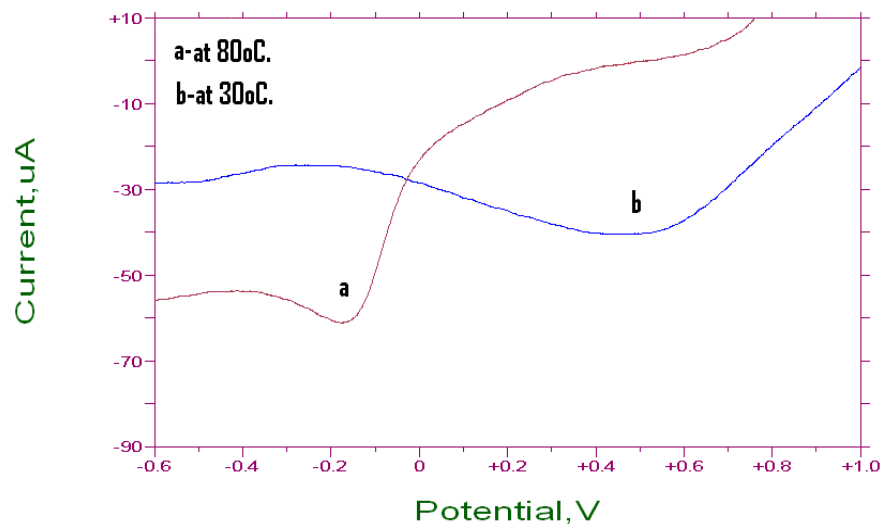

Figure 6. voltammogram for the reduction peak of 1mM Mn^{2+} in 0.1M KCl, using $C_{60}/Li^+/GCE$ versus Ag/AgCl at (a) 80^oC and (b) 30^oC, 100 mV s^{-1}.

From slope of linear relationship the value of activation energy of Mn(II). E_a is 5.07 KJ/mol compared with another work of E_a=45.35 KJ/mol [18]. The conductivity of C_{60}/Li^+ with increasing temperature also plays a significant influence on the activation energy for diffusion of the substrate of interest.

Figure 6 shows that an increase in temperature from 30 to 80^oC is accompanied by an increase in current, and causes shifting of reduction potential towards origin and in a negative direction. Evidently, simultaneous application on the use of C_{60}/Li^+, and temperature increase, exerting electrocatalytic effect [19, 20] and thermal effect respectively leads to a much higher current enhancement as observed.

3.2.3. Effect of varying scan rate

A reasonably linear dependence of Mn^{2+} reductive current on scan rate is described by y=0.4846X – 1.2069, R^2 =0.92. The slope of graph Log plot (Figure 7) is 0.48 which is quite comparable with theoretical slope of 0.5 for diffusion controlled process.
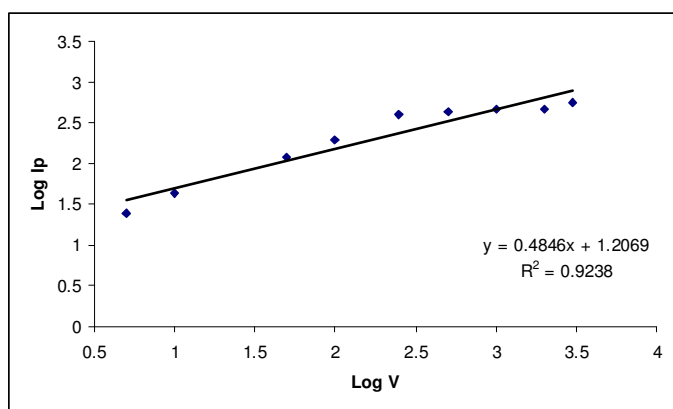

Figure 7. Plot of Log I_{pc} versus Log v, scan rate of 1mM $MnCl_2$ in 0.1M KCl using $C_{60}/Li^+/GCE$ versus Ag/AgCl.
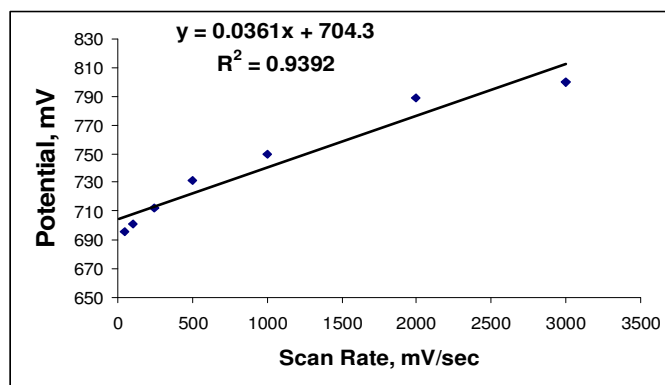

Figure 8. Plot of Potential versus scan rate of 1mM $MnCl_2$ in 0.1M KCl using $C_{60}/Li^+/GCE$ versus Ag/AgCl.

Figure 8 shows the relationship between reductive potential and scan rate of Mn^{2+}, reduction peak of 669mV at low scan rate (5mV/sec) is increased linearly to 800mV at high scan rate (1000mV/sec) as described by Y=0.0361X+704.3 (R^2=0.93). Intercepts at zero current or scan rate produces zero current potential ($E^{0, 1}$) of 704mV for the reduction of Mn(II) ion at C_{60}/Li^+/GCE.

3.2.4. Calibration Graph

Figure 9 shows the calibration curve of Mn^{2+} in different concentration (0.1-1 mM) in 0.1M KCl. Linearity of the plot of up to a Mn^{2+} concentration of 10^{-1} mM with a current sensitivity of close to 43.85μA/mM was observed with curvature being detected at a concentration of greater than 10^{-1} mM.

The calibration plots were performed at the C_{60}/Li^+/GCE in the Mn^{2+} with a good linearity of cathodic current versus Mn^{2+} as described by Y= 61.93X+43.85, R^2=0.9249. The detection limit of the method based on C_{60}/Li^+ modified GC electrode for the determination Mn(II) ion was found to be 9.2×10^{-6}M.

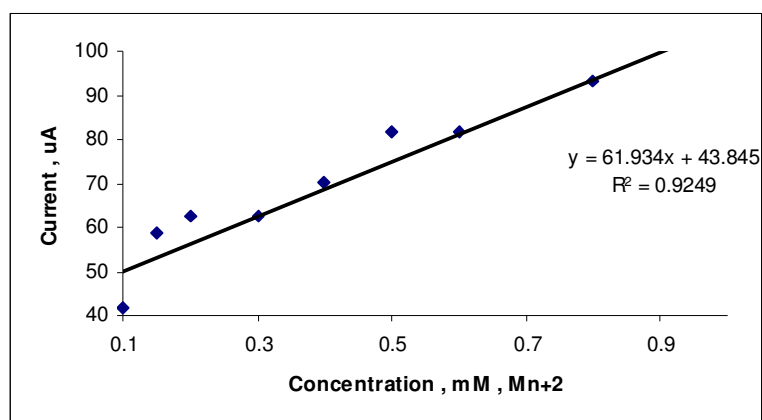**Figure 9.** Plot of reduction current versus different concentration of $MnCl_2$, 0.01-1mM in 0.1M KCl using C_{60}/Li^+/GCE versus Ag/AgCl.

3.3. Interference study

Effect of heavy metals

Possible interference of some metals in the voltammetric determination of 2mM Mn^{2+} was studied by addition of the interfering ion to a solution containing 2mM of Hg^{2+} , Cd^{2+} and Cu^{2+} using the optimized conditions at pH 2. The results in table 1 show positive interference of Hg^{2+}, Cd^{2+} and Cu^2 on the reduction peak of Mn^{2+}.

The interfering effect were investigated for metal ions in pH 2 with Mn^{2+} using the modified electrode C_{60}/Li^+/GC. The two peaks of Mn^{2+} when added to 2mM Hg^{2+} causes to shift the first reduction peak from +700 to 800mV and second reduction peak from 200 to 0mV with two folds

increase in current. In contrast, the interfering of Cd^{2+} on reduction peaks of Mn^{2+} decreased the current for both reduction peak and shifting the second peak to 0mV potential, also when used Cu^{2+} causes the same interferences to decrease the current for the first peak and shifted to lower potential, but the second reduction current peak increased four folds and shifted to high lower negative potential. It appears that Hg^{2+} ion, as in the case of C_{60}; also take part in the electro-catalysis for the reduction of Mn^{2+} to Mn.

Table 1. Effect of different heavy metals on reduction peaks of 2mM Mn^{2+} at pH 2 using $C_{60}/Li^+/GCE$ versus Ag/AgCl.

Heavy Metals	$Ip_c(I)$, µA	$Ip_c(II)$, µA	$Ep_c(I)$, mV	$Ep_c(II)$, mV
Mn^{2+}, 2mM	-300	-150	+700	+200
Hg^{2+}, 2mM	-380	-320	+800	0
Cd^{2+}, 2mM	-60	-54	+650	0
Cu^{2+}, 2mM	-100	-788	+450	-1220

3.4. Application Study

3.4.1. Seawater Recovery

The determination of Mn^{2+} concentration in seawater was carried using $C_{60}/Li^+/GCE$. Recoveries experiment were evaluated using direct calibration based on calibration curve. The recovery of 97.5± 5.9% was obtained after the addition of 0.05mM Mn^{+2} in to seawater as in Table 2.

Table 2. Recovery rate of 0.05mM Mn^{2+} added in to seawater using C_{60}/Li^+ modified GCE.

Number of sample	concentration of Mn^{2+} (mM)	Recovery Rate (%)	Mean Recovery %	Relative Standard Deviation %
1	0.049	90		
2	0.050	100		
3	0.052	104		
4	0.048	96	97.5	5.9

3.4.2. Analysis of Mn(II) in blood sample

The determination of Mn^{2+} concentration in blood samples (mouse blood) using $C_{60}/Li^+/GCE$. Recoveries experiment were evaluated using direct calibration of 99.6± 2.09% was obtained after the addition of 0.02mM Mn^{+2} in to blood sample as in table 3 while recovery of 99.03 ± 2.1% was obtained after the addition of 0.03mM Mn^{+2} into blood sample as in table 4.

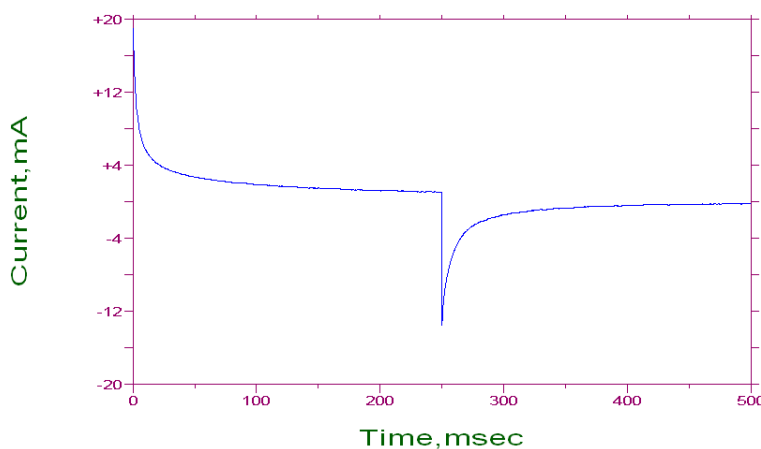**Table 3**. Recovery rate of 0.02mM Mn^{2+} added in to blood at a scan rate of 100mV/sec using $C_{60}/Li^+/GCE$.

Number of sample	concentration of Mn^{2+} (mM)	Recovery Rate (%)	Mean Recovery %	Relative Standard Deviation %
1	0.0205	102.5		
2	0.0199	99.5		
3	0.0198	99.0		
4	0.0195	97.5	99.6	2.09

Table 4. Recovery rate of 0.03mM Mn^{2+} added in to Blood at a scan rate of 100mV/sec using $C_{60}/Li^+/GC$.

Number of sample	concentration of Mn^{+z} (mM)	Recovery Rate (%)	Mean Recovery %	Relative Standard Deviation %
1	0.0305	101.6		
2	0.029	96.6		
3	0.0295	98.3		
4	0.0299	99.6	99.03	2.1

3.5. Chronoamperometry (CA) and Chronocoulometry (CC).

Figure 10 shows the monotonous rising and decaying current transient in accordance to the theoretical expectation of the Cottrell equation [21-22] based on the diffusion process to a planar electrode. Diffusion coefficient (D) of Mn^{2+} ion in 0.1 M KCl using $C_{60}/Li^+/GC$ as a working electrode is $5.12 \times 10^{-6} cm^2/Sec$. It was found that the $C_{60}/Li^+/GCE$ has a total charge transferred of 12.24 $\mu C/m^2$ in Mn^{2+} at pH=2, while the low charge transferred of 2.86$\mu C/m^2$ in Mn^{2+} at pH=8. This shows that $C_{60}/Li^+/GCE$ in acidic solution is more reducible than in alkaline solution as in Figure 11.

Figure 10. Chronoamperomogram or Cottrell plot obtained for the reduction of 1mM Mn^{2+} in 0.1M KCl as supporting electrolyte using $C_{60}/Li^+/GCE$. Potential was scanned in a negative direction from -1800 to +1800mV with 250msec. pulse width versus Ag/AgCl.
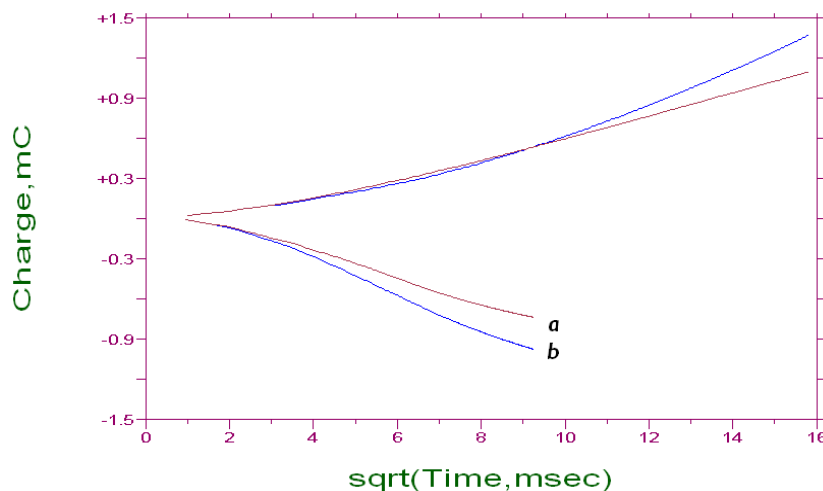
Figure 11. CC or Anson plot of charge versus $t^{1/2}$ obtained for the reduction of 1mM $MnCl_2$ and 0.1M KCl at (a) pH 8 and (b) pH 2 using $C_{60}/Li^+/GCE$ versus Ag/AgCl.

4. CONCLUSIONS

A C_{60} modified glassy electrode has been successfully fabricated by using solution evaporation method with and without Li^+ dopant. The results show conclusively that $C_{60}/Li^+/GCE$ is able to mediate more effectively in the electro-reduction of Mn^{2+} with significant current enhancement. In general, the two reduction peaks of Mn^{2+} are dependent on the concentration, scan rate, pH and temperature. Based on, interference studies with heavy metal ions, Hg^{2+}, Cu^{2+} and Cd^{2+} were found to post positive interferences on the reduction of Mn^{2+} to Mn^0.

The usefulness and reliability of $C_{60}/Li^+/GCE$ in the determination of Mn^{2+} in solution is ascertained by excellent recovery values and low relative standard deviation obtained for samples containing a known concentration of Mn^{2+} to seawater and mouse blood.

The magnitude of the surface charge determined by Anson's plot shows that $C_{60}/Li^+/GCE$ modified glassy electrodes doping is more conductive (large current transferred) as compared with C_{60}/GCE and GCE. Diffusion Coefficient and activation energy have been determined voltammetrically for the reduction of Mn^{2+} at $C_{60}/Li^+/GCE$.

References

1. W.T. Tan, A. M. Bond, S. W. Ngooi, E.B.Lim and J. K. Goh, *Anal. Chim. Acta*, 491 (2003) 181.
2. M. Nishizawa, K. Tomura, T. Matsue and I. Uchida, *J. Electroanal. Chem.* 379 (1994) 233.
3. S. A. Lerke, D. H. Evans and P. J. Fagan, *J. Electroanal. Chem.* 383 (1995) 127.
4. R. G. Compton, R. A. Spaman, D. J. Riley, R. G. Wellington, J. C. Eklund and A. C. Fisher, *Electroanal. Chem.* 344 (1993) 235.

5.   R. N. Goyal and S. P. Singh, *Electrochim. Acta.* 51 (2006) 3008.
6.   S.V. Lokesh, B.S. Sherigara, Jayadev, H.M. Mahesh and R. J. Mascarenhas, *Int. J. Electrochem. Sci.*, 3(2008)578-587.

7.   L. Xiao, G. G. Wildgoose, A. Crossley and R. G. Compton, *Sensors and Actuators B* 38 (2009) 397.
8.   A. Szucs, A. Loix, J. B. Nagy and L. Lamberts, *J. Electroanal. Chem.* 397 (1995) 191.
9.   W. W. Pai, , C. L. Hsu, C. R. Chiang, Y. Chang and K. C. Lin, *Surface Sci.* 519 (2002) 605.
10. W. T.Tan and J. K.Goh, *Electroanalysis* 20 (2008) 2447.
11. W. T. Tan, E. Lim and A. Bond, *J. Solid State Electrochem.* 7 (2003) 134.
12. M. Karabaliev and V. Kochev, *J. Electroanal. Chem*. 571 (2004) 73.
13. Y. Murayama, B. Weber, K. S. Saleem, M. Augath and N. K. Logothetis *J.M. R. I.* 24 (2006) 349.
14. M. Karabaliev and V. Kochev, *Electrochem. Comm*. 4 (2002) 857.
15. F. Scholz and B. Lange, *Trends in Analytical Chemistry*, 11 (1992) 359.
16. W. T. Tan, G. K. Ng and A. M. Bond, *Malaysian J. Chem.* 2 (2000) 34.
17. F. A. Cotton and G. Wilkinson, *Advanced Inorganic Chemistry*, Fifth edition, John Wiley and Sons (1988).
18. V. Thangadurai, A. K.Shukla and J. Gopalakrishnan, *J.Chem. Commun.* 116 (1998) 2647.
19. K.Q.Ding, *Int. J. Electrochem. Sci.* 5(2010) 72-87.
20. J. P. Singh, X. G. Zhang, Hu -lin Li, A. Singh and R.N. Singh, *Int. J. Electrochem. Sci.*, 3(2008) 416 – 426.
21. Instruction manual, CV 50W, version 2, Bioanalytical system Inc. USA (1996).
22. A. J. Bard, L. R. Faulkner, *Electrochemical Methods: Fundamentals and Applications*, 2nd Ed. Wiley, New York (2001).